

Perturbed Structure of Molecular Hydrogen near the Second Dissociation Limit

E. F. McCormack

Argonne National Laboratory, Argonne, Illinois 60439

E. E. Eyler

Department of Physics and Astronomy, University of Delaware, Newark, Delaware 19716

(Received 3 December 1990)

The region of the second dissociation limit of H_2 converging to $H(1s) + H(2s, 2p)$ has been investigated using high-resolution double-resonance spectroscopy through the $E, F^1\Sigma_g^+$ state. Transitions to the very high vibrational levels of the $B^1\Sigma_u^+$, $B'^1\Sigma_u^+$, and $C^1\Pi_u$ states have been measured with 0.02-cm^{-1} accuracy. Numerous perturbations and unexpected transitions are observed as far as 10 cm^{-1} below the dissociation limit. This complex structure, still not fully understood, arises from a combination of electronic, fine-structure, and hyperfine interactions.

PACS numbers: 33.80.Rv, 34.20.Cf

The region very near a molecular dissociation threshold is a unique physical regime where long-range interatomic potentials dominate. Typically the adiabatic potential curves are very accurately known and are fully described by the first few terms of a power-series expansion in the internuclear separation. In this adiabatic picture both the highest bound vibrational levels and the continuum just above threshold are easily calculated, and simple theoretical models have been developed to parametrize the vibrational spacings.^{1,2} However, extensive perturbations or even a complete reordering of the vibrational spectrum can occur when the vibrational spacing becomes comparable to the energy separation between different electronic states converging to the same limit, or when the vibrational spacing approaches the scale of the fine and hyperfine structures of the dissociating atoms. Some of these effects have been investigated in high-resolution studies of heavy diatomic molecules, particularly I_2 and Cs_2 .³

In this paper we describe the first high-resolution study of the threshold region in H_2 , including extremely long-range vibrational levels with binding energies as small as 0.2 cm^{-1} and outer turning points in excess of 100 bohrs. For such weakly bound states the perspectives of molecular physics and atomic collision theory are almost equally applicable. Recent investigations of cold and ultracold collisions of alkali-metal atoms in atom traps have revealed partially resolved resonant structure thought to arise from analogous weakly bound molecular levels.⁴ Some of the unusual spectra and interactions described here will probably be typical of these other one-electron systems as well.

In our experiment optical double resonance is used to excite the ungerade (*u*) states converging to $H(1s) + H(2l)$. As shown in Fig. 1, bound and continuum levels of the $B^1\Sigma_u^+$, $B'^1\Sigma_u^+$, and $C^1\Pi_u$ states are excited by a high-resolution laser from the $E, F^1\Sigma_g^+$ state. In the adiabatic approximation, the $B'^1\Sigma_u^+$ state correlates to $H(1s) + H(2s)$, while the *B* and *C* states correlate to $H(1s) + H(2p)$. Transitions to the rovibrational levels of

all three states are possible, though the adiabatic electronic transition moments to the *B* state are orders of magnitude weaker than to the *B'* or *C* state.⁵ The *B* state is quite unusual because its broad resonant $1/R^3$ potential curve supports a relatively dense set of high vibrational levels.

The adiabatic picture breaks down for two reasons. First, nonadiabatic couplings extensively mix the electronic configurations of the *B*, *B'*, and *C* states. This mixing is apparent both in experimental results, where very strong transitions to the *B* state are observed, and in nonadiabatic calculations of numerous bound levels by Senn, Quadrelli, and Dressler.⁶ Second, a complete description of the region very near threshold must include the fine and hyperfine interactions, as well as the 0.035-cm^{-1} Lamb-shift splitting between the $2s$ and $2p$ atomic limits. Such a calculation has not yet been undertaken, although a recent analysis of $2s:2p$ branching

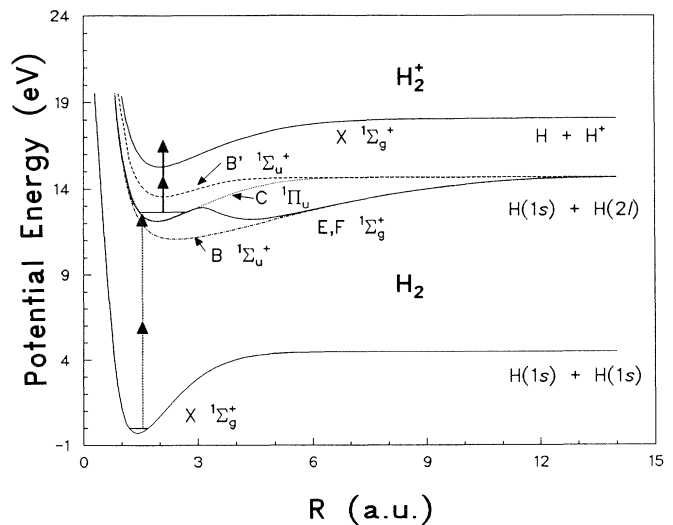


FIG. 1. Adiabatic potential-energy curves of selected electronic states near the second dissociation limit of H_2 .

ratios in the continuum included some of these interactions.⁷

Transitions to high-lying levels of the B , B' , and C states have previously been observed in absorption by several groups, most recently using vacuum-uv radiation generated from a dye laser.^{8,9} Close to threshold, spectral resolution limited to at best 0.1 cm^{-1} has caused problems with spectral overlapping and ambiguous assignments. This region also has been observed in double-resonance spectroscopy through the $\nu=5$ and 6 levels of the E, F state, but individual levels were not resolved.¹⁰ Stwalley¹ has used a WKB model developed by LeRoy and Bernstein² to analyze the high vibrational levels of the B state, based on data obtained by Herzberg.⁸ However, as we shall discuss below, the adequacy of this simple model very close to threshold is questionable.

In our experiment, the $E, F^1\Sigma_g^+$ state is populated by two-photon excitation, with somewhat different arrangements for populating the $\nu=3$ and 6 levels. For $\nu=3$ we obtain $10\text{-}\mu\text{J}$, 10-ns laser pulses at 197 nm by mixing the second harmonic of a 591-nm dye laser with its fundamental in a $\beta\text{-BaB}_2\text{O}_4$ crystal thermoelectrically cooled to -30°C . To excite the $\nu=6$ level, $100\text{-}\mu\text{J}$ laser pulses at 193 nm are generated by mixing the fourth harmonic of a Nd-doped yttrium aluminum garnet (Nd:YAIG) laser at 266 nm with a Nd:YAIG-pumped dye laser at 705 nm , with room temperature $\beta\text{-BaB}_2\text{O}_4$.

In the "probe" step, the threshold region is excited from the E, F state by a pulse-amplified cw laser producing 10-nsec , 3-mJ pulses with a bandwidth of about 0.003 cm^{-1} . The wavelength is approximately 594 nm when starting from the $\nu=3$ level of the E, F state, or 677 nm from $\nu=6$. Bound levels are by resonant two-photon ionization, in which a second red photon produces H_2^+ , H^+ , or H^- ions. The photodissociation continuum can also be observed by collecting Lyman- α photons from the resulting H atoms.

A molecular beam of H_2 is formed from a pulsed supersonic expansion and collimated to give a residual Doppler width of 250 MHz . The weakly focused lasers cross the molecular beam at right angles 20 cm from the nozzle. A pair of electric-field plates is used to collect either positive or negative ions with a typical field of 300 V/cm . H_2^+ and H^+ ions are easily distinguishable by their time of flight to the detector. The absorption spectrum of I_2 at 250°C is used for wavelength calibration.

The energy region from 0 to 40 cm^{-1} below threshold was studied systematically. In parahydrogen ten transitions from the $\nu=6$, $N=0$ level of the E, F state were observed. In orthohydrogen we observed ten transitions from the $\nu=3$, $N=1$ level and fourteen transitions from $\nu=6$, $N=1$. Of these, nine pairs of transitions share a common upper level. Most of the measurements were made by detecting H^+ ions, but resonant signals were observed in all three possible ion channels: H_2^+ , H^- , and H^+ . The production of all three species indicates

the complex dynamical behavior of the final continuum states produced in the resonant multiphoton excitation process. These highly unstable states can decay by autoionization into $\text{H}_2^+ + e^-$, by dissociation into the ion pair $\text{H}^+ + \text{H}^-$, or by dissociation into $\text{H}(1s) + \text{H}(nl)$ atoms that can subsequently be ionized.¹¹

Although the branching ratios between the ionic channels have yet to be studied carefully, the results obtained so far indicate that the yields of H^+ and H_2^+ are roughly equal. There is no significant variation in the relative yields over most of the energy range studied, with the notable exception that the onset of a large continuum is seen in the H^+ channel, starting just below the dissociation limit. This continuum, into which the highest vibrational levels are blended, is clearly visible in the typical spectrum shown in Fig. 2. The spectrum observed in the H^- channel is very similar to that in the H^+ channel and is very roughly 10 times weaker, although this ratio was not accurately measured.

The transition wavelengths were measured for several laser powers and extrapolated to their zero-power values. Extrapolations were performed by assuming both linear and square-root dependences on the laser intensity.¹² The average of the two results was used for the final value, and the difference between them was used to estimate the uncertainty in the extrapolation. The transition energies measured at the lowest laser power were within 0.01 cm^{-1} of the final extrapolated value. The results are given in Table I, with uncertainties that include both the systematic error from this power extrapolation and a wavelength measurement uncertainty of 0.01 cm^{-1} due to scan nonlinearities and uncertainty in the I_2 atlas.¹³

Absolute term energies relative to the ground state can be found from Table I by adding the E, F -state term en-

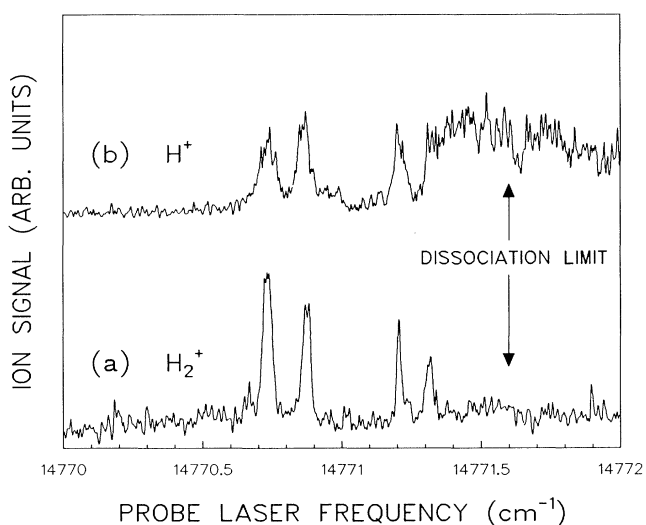


FIG. 2. Spectrum obtained from the $\nu=6$, $N=1$ level of the $E, F^1\Sigma_g^+$ state by detecting (a) H_2^+ and (b) H^+ . The weakest level shown in Fig. 3 is unobservable in this scan.

TABLE I. Transitions excited from the $E, F^1\Sigma_g^+$ state.

$\nu=3, N=1$	$\nu=6, N=0$	$\nu=6, N=1$
16810.210(14)	14783.539(11)	14731.237(12)
16812.467(15)	14813.829(11)	14735.101(12)
16812.605(15)	14813.882(11)	14738.624(15)
16818.941(17)	14816.583(11)	14744.059(11)
16818.972(17)	14816.795(12)	14760.899(15)
16819.831(16)	14816.955(10)	14761.003(15)
16819.980(15)	14817.217(11)	14767.367(15)
16822.12(20) ^a	14817.313(11)	14767.400(15)
16822.331(15)	14817.340(11)	14768.269(15)
16822.812(15)		14768.381(15)
16822.936(15)		14770.751(12)
		14770.894(10)
		14771.225(16)
		14771.339(15)

^aToo weak for accurate extrapolation to zero power.

ergies. We have previously measured the $\nu=3, N=1$ level, obtaining $101\,554.041 \pm 0.010 \text{ cm}^{-1}$.¹⁴ The term energy for $\nu=6, N=1$ can be calculated from $\nu=3$ by using combination differences from Table I, with a result of $103\,605.623 \pm 0.018 \text{ cm}^{-1}$. Finally, the energy for $\nu=6, N=0$ is calculated using the $N=0-1$ rotational interval given by Dieke,¹⁵ accurate to about 0.03 cm^{-1} , giving $103\,559.633 \pm 0.035 \text{ cm}^{-1}$.

Stick diagrams in Fig. 3 show the binding energies of the observed levels closest to the dissociation limit, together with previously assigned levels of the B' and C states as given by Senn, Quadrelli, and Dressler⁶ and the predicted positions of the highest B -state levels given by Stwalley.¹ All possible singlet ungerade levels in this energy region are included in the predicted spectrum. The line heights indicate the relative sizes of the observed transitions. We also observed five transitions to lower-lying levels not shown in Fig. 3; they agree well with calculated energies and confirm the strong mixing between the $B, \nu=36$ level and the $B', \nu=8$ level predicted by the nonadiabatic calculations of Senn, Quadrelli, and Dressler. The predicted and observed spectra begin to differ significantly about 12 cm^{-1} below threshold, at first with the appearance of extra lines in at least four cases, and finally with a complete breakup of the vibrational sequence in the last 1 cm^{-1} .

The irregular behavior within 1 cm^{-1} of the limit is to be expected, because the vibrational spacing in this region is comparable in scale to the fine-structure and Lamb-shift interactions in the $n=2$ H atom. The double lines seen for several much more strongly bound levels of the B state are more surprising and can only arise from admixture of the singlet ungerade levels with other levels that are nearly degenerate. The repeated occurrence of this doubling suggests that the degeneracy occurs regularly, implying that the perturbing state must have a long-range potential curve nearly identical to the B state. A study of the interatomic potentials shows only one

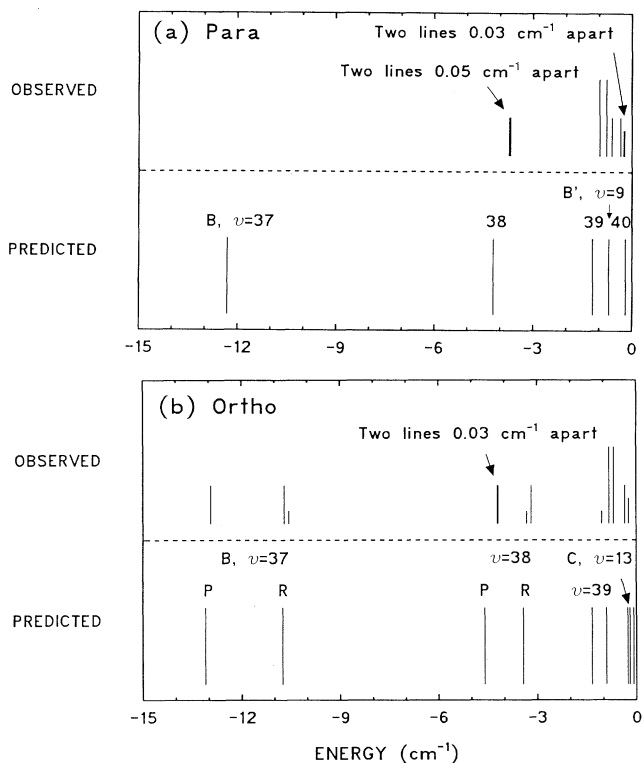


FIG. 3. (a) Comparison of observed and predicted $N=1$ levels of parahydrogen. (b) Same comparison for $N=0$ and 2 states of orthohydrogen. The binding energies are given relative to the dissociation limit, here taken to be $118\,377.2 \text{ cm}^{-1}$.

candidate, the triplet gerade (g) potential curve arising from the same $1s+2p$ limit.¹⁶

The only perturbation that can give rise to the normally forbidden admixture of these states is the hyperfine interaction. Hyperfine-induced $g-u$ mixing has been observed previously in I_2 and Cs_2 , and has been analyzed in some detail.³ The $g-u$ coupling term is typically similar in magnitude to the atomic hyperfine splitting. This term can be evaluated explicitly when the molecular wave function can be written as a simple combination of atomic wave functions (not a good approximation here because the atomic fine structure is strongly mixed). In atomic hydrogen, the $F=0$ and 1 levels of the $1s_{1/2}$ ground state are split by 0.048 cm^{-1} , in good agreement with the splittings of $0.03-0.2 \text{ cm}^{-1}$ that we observe in the molecular spectrum. A more quantitative analysis using parametrized fits as in the earlier work is not practical for H_2 because the spectrum has too few lines.

On a somewhat coarser energy scale, the B -state vibrational spacings can be compared with Stwalley's WKB model.¹ He fitted and extrapolated the high vibrational levels of the B state by using an asymptotic expression for the adiabatic energies,

$$\nu_D - \nu \cong a_3(\epsilon_\nu)^{1/6}.$$

Here ν_D is the effective vibrational quantum number at the dissociation limit, ϵ_ν the binding energy of level ν , and a_3 an easily calculated constant. It would clearly be useful to repeat his analysis with our improved energy levels. Unfortunately, it is now clear that the crucial $\nu=39$ level cannot be reliably assigned without a full analysis of fine and hyperfine interactions, and the previous assignment must be interpreted as a blended line. If the dissociation limit is calculated using $\nu=37$ and 38 (taking the average of the two closely spaced $\nu=38$ lines), a limit of 118377.8 cm^{-1} is found. For $\nu=36$ and 37 the result is 118381.8 cm^{-1} . Both values are too high compared with the theoretical value of $118377.05 \text{ cm}^{-1}$ or the experimental value of $118377.2(2) \text{ cm}^{-1}$ we have obtained by observing the onset of the dissociation continuum.¹⁷ These values are given for the $1s_{1/2} + 2s_{1/2}$ limit, but the weighted average for $2s$ and $2p_{1/2}$ is only 0.1 cm^{-1} higher. We conclude that vibrational extrapolations should be approached very cautiously, since their region of validity is often quite limited.

In summary, the observed spectra, even though sparse, show evidence for strong configuration mixing, hyperfine-induced symmetry breaking, and a complete rearrangement of the spectrum very near the limit. Because so many interactions play a significant role, they will probably have to be considered together for a successful theoretical treatment. One possibility is to employ generalized multichannel quantum-defect theory, an approach used already for theoretical studies of near-threshold behavior in alkali-metal dimers.^{4,18} Once the structure is fully understood, a precise determination of the dissociation energy by vibrational extrapolation should become possible.

Further experimental work is under way, including extension to the HD and D₂ isotopes and an investigation of the continuum just above the dissociation threshold. The development of theoretical methods for treating the near-threshold region is badly needed, and we hope that these results will encourage such an effort.

This research was supported by NSF Grant No. PHY90-00375. E.F.M. was also supported by the Department of Energy, Office of Health and Environmental Research under Contract No. W-31-109-ENG-38. We thank Robert Field and Paul Julienne for helpful conversations, and John Brandon of Interconnection Products for providing thermoelectric coolers.

¹W. C. Stwalley, Chem. Phys. Lett. **6**, 241 (1970).

²R. J. LeRoy and R. B. Bernstein, J. Chem. Phys. **52**, 3869 (1970); R. J. LeRoy, J. Chem. Phys. **73**, 6003 (1980).

³M. D. Levenson and A. L. Schawlow, Phys. Rev. A **6**, 10 (1972); J. Vigué, M. Broyer, and J. C. Lehmann, Phys. Rev. Lett. **42**, 883 (1979); J. P. Pique, F. Hartmann, R. Bacis, S. Churassy, and J. B. Koffend, Phys. Rev. Lett. **52**, 267 (1984); J. P. Pique, F. Hartmann, S. Churassy, and R. Bacis, J. Phys. (Paris) **47**, 1909 (1986); **47**, 1917 (1986); H. Weickenmeier, U. Diemer, W. Demtröder, and M. Broyer, Chem. Phys. Lett. **124**, 470 (1986).

⁴P. Lett, P. Jessen, C. Westbrook, S. Rolston, W. Philips, P. Julienne, and P. Gould (to be published); P. S. Julienne and F. H. Mies, J. Opt. Soc. Am. B **6**, 2257 (1989); J. Weiner, J. Opt. Soc. Am. B **6**, 2270 (1989).

⁵L. Wolniewicz, J. Chem. Phys. **51**, 5002 (1969); L. Wolniewicz and K. Dressler, J. Mol. Spectrosc. **96**, 195 (1982).

⁶P. Senn, P. Quadrelli, and K. Dressler, J. Chem. Phys. **89**, 7401 (1988).

⁷J. A. Beswick and M. Glass-Maujean, Phys. Rev. A **35**, 3339 (1987); M. Glass-Maujean (private communication).

⁸G. Herzberg, J. Mol. Spectrosc. **33**, 147 (1970).

⁹T. J. Namioka, J. Chem. Phys. **40**, 3154 (1964); **41**, 2141 (1964); **43**, 1636 (1965); S. Takezawa, J. Chem. Phys. **52**, 2575 (1970); I. Dabrowski and G. Herzberg, Can. J. Phys. **52**, 1110 (1974); A. Balakrishnan, V. Smith, and B. P. Stoicheff (to be published).

¹⁰D. H. Parker, J. D. Buck, and D. W. Chandler, J. Phys. Chem. **91**, 2035 (1987).

¹¹S. L. Guberman, J. Chem. Phys. **78**, 1401 (1983); M. Glass-Maujean, J. Chem. Phys. **85**, 4830 (1986); S. Arai, T. Kamosaki, M. Ukai, K. Shinsaka, Y. Hatano, Y. Ito, H. Koizumi, A. Yagishita, K. Ito, and K. Tanaka, J. Chem. Phys. **88**, 3016 (1988).

¹²J. S. Bakos, Phys. Rep. **31**, 209 (1977).

¹³S. Gerstenkorn and P. Luc, *Atlas du Spectre d'Absorption de la Molecule d'Iode, 14000-15600 cm⁻¹* (Laboratoire Aime Cotton, Orsay CEDEX, France, 1978).

¹⁴E. E. Eyler, J. Gilligan, E. McCormack, A. Nussenzweig, and E. Pollack, Phys. Rev. A **36**, 3486 (1987).

¹⁵H. M. Crosswhite, *The Hydrogen Molecule Wavelength Tables of Gerhard Heinrich Dieke* (Wiley-Interscience, New York, 1972).

¹⁶W. Kolos, Int. J. Quantum Chem. **1**, 169 (1967).

¹⁷E. McCormack, Ph.D. thesis, Yale University, 1989 (unpublished); W. Kolos, K. Szalewicz, and H. Monkhorst, J. Chem. Phys. **84**, 3278 (1986).

¹⁸F. H. Mies, J. Chem. Phys. **80**, 2514 (1984); F. H. Mies and P. S. Julienne, J. Chem. Phys. **80**, 2526 (1984).